# The University of Hamburg WERA HF Radar - Theory and Solutions

K.-W. Gurgel, H.-H. Essen, and T. Schlick

*Universität Hamburg, Institut für Meereskunde, Germany*

**Abstract.** The remote sensing group of the University of Hamburg is working on HF radar since 1980. Based on 15 years of experience with CODAR, which the University of Hamburg bought from NOAA (developed by D. Barrick), a new system called WEllen RAdar (WERA) has been designed at the University of Hamburg. The design aims to be as flexible as possible in order to allow easy adjustment to different requirements, i.e. working range, spatial resolution and antenna configurations. The first part of this paper describes the technical solutions available to achieve resolution in range and azimuth. Modulation techniques for range resolution like Pulses and Frequency Modulation (FMCW) are compared, as well as Direction Finding and Beam Forming for azimuthal resolution. A short introduction in the algorithms needed is given. The second part discusses the hardware and software components available from the WERA "kit", to put together an HF radar adopted to the requirements of the actual application.

## 1 Introduction

In 1980, one year after the Marine Remote Sensing (MARSEN) Experiment [2], the University of Hamburg Remote Sensing Group started working on HF radar. In close cooperation to the HF radar group at NOAA[1], at that time lead by D. Barrick[1], three Coastal Ocean Dynamics Application Radars (CODAR) systems have been purchased. The NOAA-CODAR is completely different from the actual SeaSonde which is now delivered from CODAR Ocean Sensors. It uses a Continuous Wave (CW) pulsed modulation scheme for range resolution and 4 receive antennas arranged in a sqare for azimuthal resolution.

The first experiment with the University of Hamburg CODAR took place in 1981 on the island of Sylt, Germany [3]. Until 1983, several modifications have been done to improve the sensitivity. The working has been changed in order to reduce the impact from radio interference due to ionospheric reflections. At that time, the solar cycle was near to it's maximum and the high sun spot activity heated the ionosphere more intensively, which tended to reflect even signals in the high shortwave band between 25 MHz and 30 MHz.

In autumn 1983, the Canadian Memorial University of Newfoundland organized an "International Workshop on the Remote Sensing of Oceanic Variables Using HF Groundwave Radar" in St. John's. On this workshop E. D. R. Shearman presented results from his PISCES HF radar system, which used Frequency Modulated Interrupted Continuous Wave (FMICW) modulation for range resolution [6] and a large linear array of receiving antennas. Due to the low working frequency around 9 MHz, the working range of this system was as large as 150 km for ocean wave measurements and even more for currents.

In the next years, several tests and simulations on different techniques for range resolution lead to the conclusion that FMCW modulation may have some advantages compared to CW pulses. Some difficulties in dealing with distorted antenna patterns, especially on board of ships, have also been identified. These topics are discussed in the next sections in more detail. Based on the results of these investigations, the University of Hamburg WEllen RAdar (WERA) HF radar has been developed in 1996 [4], [5].

## 2 Techniques for spatial resolution

Radar stands for **Ra**dio **d**etection **a**nd **r**anging. A target should not only be identified, it should also be determined in range and azimuth. Several different techniques have been developed during the past 50 years, mainly for navigation purposes. In remote sensing applications, the aim is to measure geophysical parameters. The processing of the radar echos has to be modified, e.g. timeseries at a specific position have to be acquired instead of tracking a target. However, the basic ideas are quite similar. The next sections discuss different techniques for range and azimuthal resolution in a remote sensing radar.

### *2.1 Range resolution by CW pulses*

The CODAR uses coherent CW pulses for range resolution. The length of the pulse determines the spatial resolution in range, e.g. a pulse with a duration of 8 $\mu s$ corresponds to a 1.2 km wide circle around the radar. The radio bandwidth $B$ required for this resolution is $B = 1/(8\,\mu s) = 125$ kHz.

Figure 1 shows the timing used within the CODAR. After transmitting the pulse, the received signal is sampled to form the consecutive range cells, the range incre-

[1] National Oceanic and Atmospheric Administration, USA

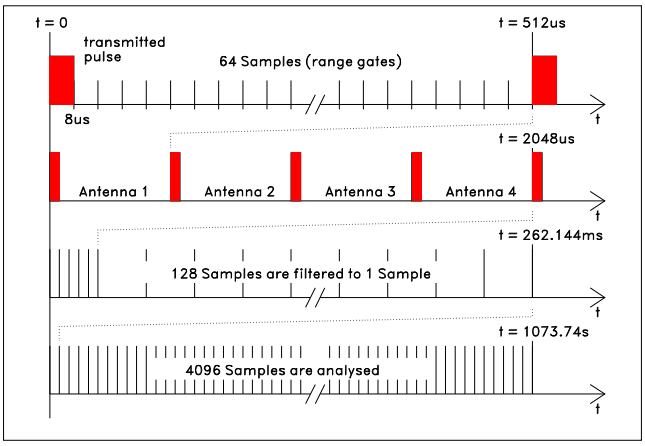


**Figure 1.** The timing used within the CODAR.

asing with the time delay from the transmitted pulse. As the expected echo strength decreases with range, the receiver gain can be increased as a function of range to overcome dynamic range limitations. 4 receive antennas are multiplexed to allow azimuthal resolution, giving a total length of one cycle of 64 range cells times 4 antennas times 8 $\mu s$. 128 of these cycles are averaged together in a digital filter and form the first sample of the 64 by 4 time series. After about 18 minutes, 4096 samples have been acquired in each time series.

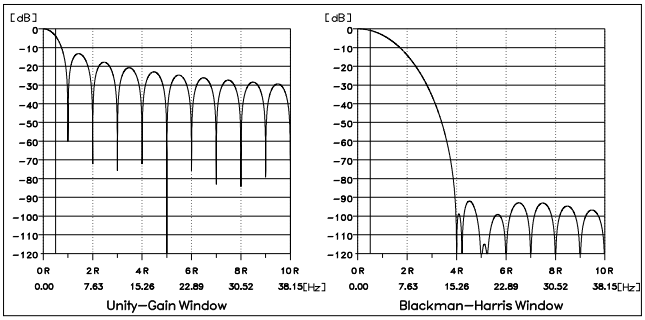


**Figure 2.** The frequency response of the digital filter used in the CODAR with a unity-gain and a Blackman-Harris window applied. All signals at frequencies higher than 0.5 $R$ are aliased back.

The bandwidth of the analog signal is 125 kHz to allow for the required range resolution and the effective sampling rate for a specific range cell and antenna is $R_{eff} = 1/(2048\ \mu s) = 488.3$ Hz. Thus, aliasing can not be avoided by a matching analog low pass filter. There is no radar signal expected in this aliased frequency range, however noise and interference can not be suppressed.

Signals below $0.5 \cdot R_{eff}$ can be attenuated by the digital filter. The sample rate at the output of this filter is $R = 1/(128 \cdot 2048\ \mu s) = 3.815$ Hz. Figure 2 shows the frequency response of the digital filter for a unity-gain window and a Blackman-Harris window. The sampling rate $R$ has to be selected high enough to cover the frequency range of the expected sea echos. Signals above $0.5 \cdot R$ are aliased back into the spectrum of the sea echos. The Blackman-Harris window offers a better suppression of noise and interference for frequencies above $0.5 \cdot R$ compared to the unity-gain window.

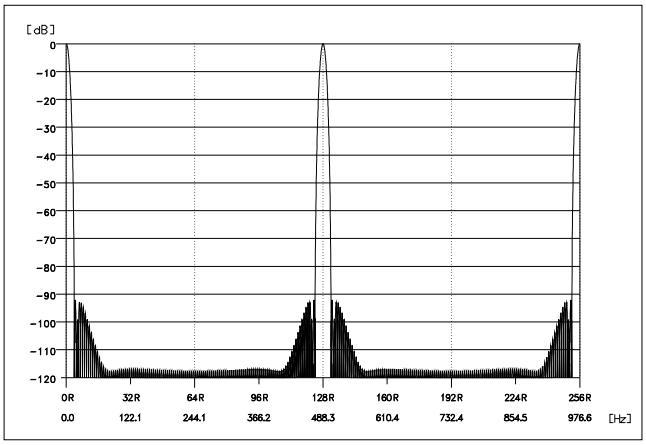


**Figure 3.** The frequency response of the digital filter used in the CODAR up to 256 $R$ with a Blackman-Harris window applied.

Figure 3 shows the signal attenuation as a function of frequency at the output of the digital filter for a Blackman-Harris window up to $256 \cdot R$. The frequency response of the digital filter is repeated around multiples of $R_{eff} = 128 \cdot R$ until the analog low pass filter starts to attenuate the input signal. There are 256 of these aliased frequency bands, which at least contain thermal and athmospheric noise. Adding up these noise bands reduces the signal-to-noise ratio by 24 dB. The reason behind this is a bandwidth of $\geq 125$ kHz required for sufficient range resolution and at the same time of $\leq 300$ Hz to avoid aliasing. The frequency responses of the digital filter and the sampling method of the CODAR shown in figures 2 and 3 have been simulated numerically and measured in the lab by using a signal generator.

The problem described above is a basic constraint valid for all pulsed radar systems. On the other hand, an echo is sampled into the correct range cell, even if it comes from a target with a Doppler shift above Nyquist, e.g. a ship at high speed. In this case the echo is aliased back and appears at the wrong Doppler shift. As shown later, FMCW modulation will move the echo to a wrong range cell.

### *2.2 Range resolution by FMCW*

Performing the range resolution in frequency domain, solves some of the problems described above. By using a continuously transmitted signal, which is linearily increasing (or decreasing) in frequency with time, a target producing an echo at a time delay $\Delta t$ will appear at a frequency offset of $\Delta f$ (figure 4). This frequency offset is constant with time, except during the time from 0 to $\Delta t$, where a high negative frequency shift from the preceding chirp can be observed. The frequency of the chirp starts at $f_0$ and increases to $f_0 + B$ during the time $T$, $B$ being the bandwidth of the chirp. This process maps a target at the distance $r$ to a frequency offset

$$\Delta f = \frac{B}{T}\frac{2r}{c}$$

with $c$ beeing the speed of light. As there is no transmit to receive switching involved, the receiver must be capable to process the strong signal from the direct path (transmit antenna to receive antenna) and the weak signals from far ranges simultaneously.

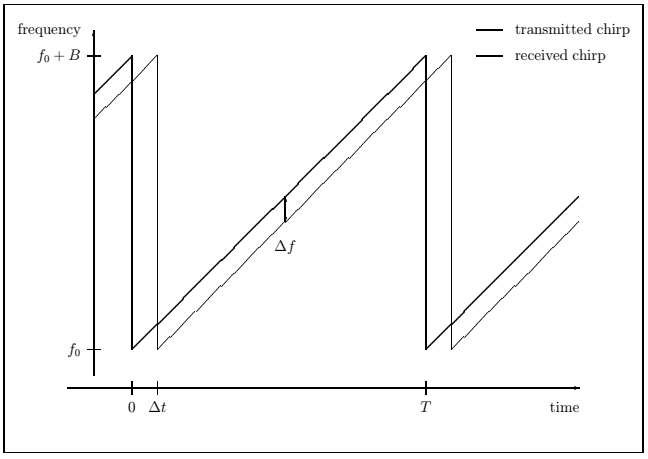


**Figure 4.** A linear frequency chirp starting at $f_0$ with the bandwidth $B$ and a duration $T$. After reaching the end frequency $f_0+B$, the chirp phase contiguously starts again at $f_0$.

The linear frequency chirp can be generated by Voltage Controlled Oscillators (VCO) or Direct Digital Synthesizers (DDS). As of the year 2000, the DDS technique can produce extremely linear and low sideband-noise chirps at frequencies up to 100 MHz, directly covering the working frequencies of HF radars. In the microwave radar bands, VCO techniques or a complex frequency-doubling and -mixing scheme have still to be used.

The DDS synthesizes the output frequency from digital numbers using a Digital to Analog converter. The

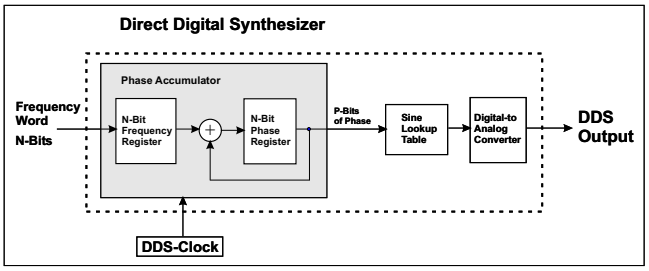


**Figure 5.** The block diagram of Direct Digital Synthesizer (DDS)

numbers are generated through a phase value to sine value lookup table. The actual phase values are calculated by adding phase increments to a phase accumulator. With each DDS clock, a phase increment value (the frequency word) is added to the actual phase. The output frequency can be adjusted by changing the frequency word or the DDS clock. Normally the DDS clock is fixed to about three times the maximum output frequency to be generated to avoid aliasing. By increasing the frequency word with each clock, a linear frequency chirp

$$S(t) = sin(2\pi(f_0 + \frac{B}{2T}t)t + \Phi_0)$$

can easily be generated. The same technique to generate frequency chirps has been used for numerical simulations shown later in this paper.

An often asked question is "how can frequency shifts due to a range offset be separated from frequency shifts due to Doppler"? The following section tries to bring some light onto this "myth".

The measurement of Doppler spectra at specific range cells using FMCW involves the following steps: To get the frequency shift $\Delta f$, the received signal is demodulated (technically speaking) or multiplied (mathematically speaking) with the actual value of the transmitted chirp. Then, a Fast Fourier Transform (FFT) is applied to the samples of one demodulated chirp. The spectral lines of this range resolving FFT are quantized to

$$\Delta f_{quant} = \frac{1}{T} = \frac{B}{T}\frac{2r_{quant}}{c}$$

The number of samples is related to the number of range cells processed, however the range cells on the "wrong" side of the spectrum contain no information: At chirps with increasing frequency, the echos always appear at negative frequency shifts $\Delta f$. There is no signal except noise and interference within the positive spectral lines. With $n$ samples taken during the first frequency chirp, $n/2$ range cells are processed. In terms of range cell width, this frequency quantization corresponds to

$$r_{quant} = \frac{c}{2B}$$

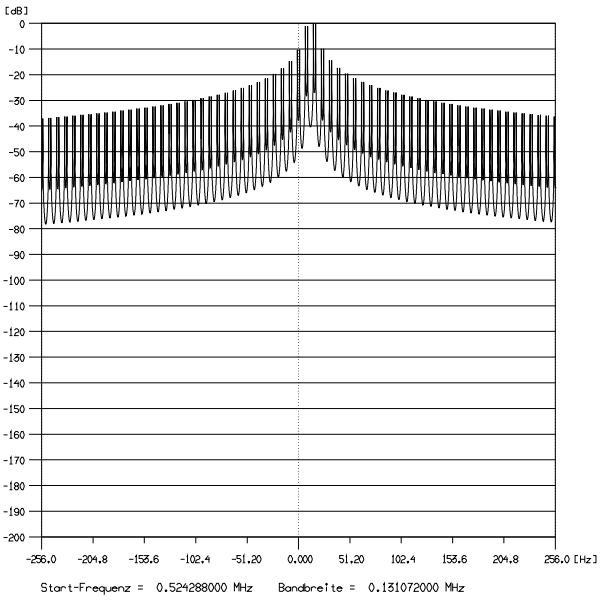


**Figure 6.** Simulation result: Sea echos at ±1.1 Hz positioned at range cell $1+\frac{17}{32}$. Due to the phase incontiguity, this signal also appears at neighbouring range cells.

An analog lowpass filter with a cut-off frequency of $(n/2) \cdot \Delta f_{quant}$ can be used to avoid any aliasing due to sampling below Nyquist frequency. In practice, by processing $k$-times more range cells than required, $k$-times oversampling can be used do reduce quantization noise due to the limited resolution of the A/D converter. It is essential that all sampling is done simultaneously to the frequency chirps. A range resolution $r_{quant} = 1.2$ km again requires a bandwidth $B = 125$ kHz.

Range resolving FFTs are now calculated on consecutive chirps, tracking the phase variation of the signal at a given range cell. The processing of $m$ chirps forms a time series of $m$ samples for each range cell. By applying a Fourier transform to these time series, the Doppler spectrum for a given range cell can be calculated.

A problem arising with the range resolving FFTs is caused by the phase incontinuity from the last sample to the first sample of the chirp. Numerical simulations have been used to demonstrate the severity of this problem. The frequency chirp has been calculated using the DDS technique desribed above. The following parameters have been used for the simulation: Clock frequency of the DDS $f_{clock} = 2^{22}$ Hz, start frequency of the chirp $f_0 = 2^{19}$ Hz, bandwidth $B = 2^{17}$ Hz, duration $T = 2^{-3}$ s $= 0.125$ s. The two Bragg lines caused by the scattering ocean waves have been set to ±1.1 Hz. 128 chirps have been processed. By shifting the time delay $\Delta t$, the echo was adjusted to range cell $1 + \frac{17}{32}$, which is nearly between two range cells and a 'worst-case' situation. The result of this simulation can be seen in figure 6.

Depending on working frequency, water salinity and sea state, the power of the sea echos decreases at 1 to 3 dB per range cell. The most powerful signals reflected from the sea surface appear at the first range cells. These signals are smeared out and dominate the far range cells. This effect prevents the radar to resolve the echos from far range cells. The solution is to apply a windowing function to the samples of each chirp prior to the range resolving FFT. This window slightly reduces the selectivity in the two neighbouring range cells, but it strongly reduces these signals at far range cells. Figure 7 shows the distribution of the smeared signals when a Blackman-Harris window is applied prior to the range resolving FFT.

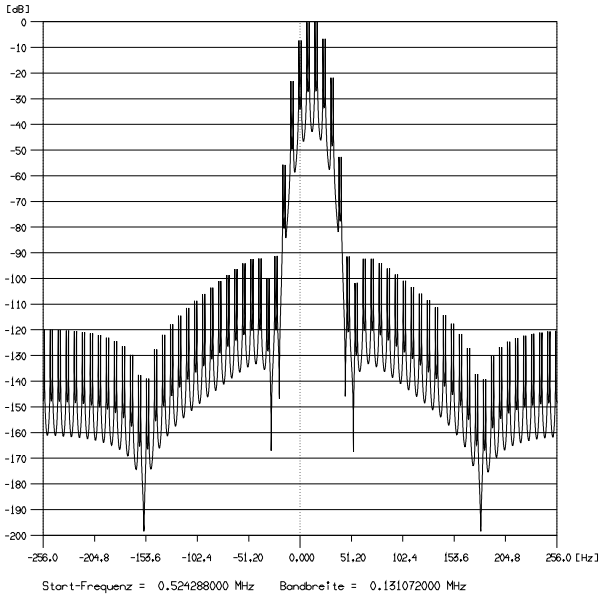


**Figure 7.** Simulation result: Sea echos at ±1.1 Hz positioned at range cell $1+\frac{17}{32}$. After applying a Blackman-Harris window, range smearing is strongly reduced.

Like in the pulsed range resolution scheme, the process described above also does not handle correctly signals with Doppler shifts above Nyquist frequency $T/2$ within a range cell. In case of FMCW however, these signals appear at the wrong Doppler shift **and** the wrong range cell. Numerical simulations of frequency chirps increasing nonlinearily with time have shown additional range smearing.

### *2.3 Azimuthal resolution by Direction Finding*

The two different techniques to resolve the incident angle of a sea echo are Direction Finding and Beam For-

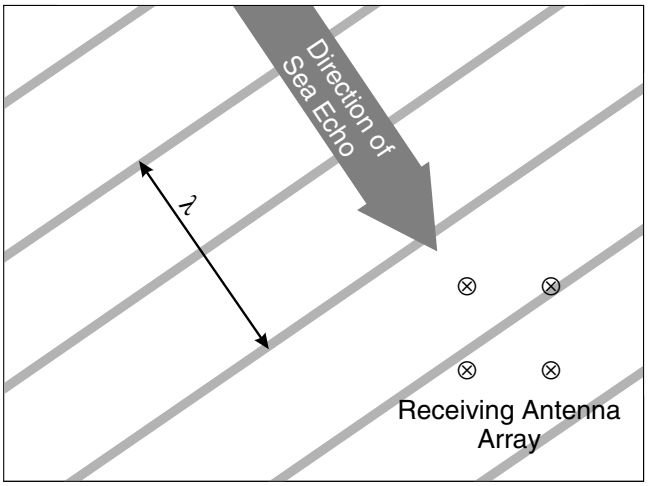


**Figure 8.** A sea echo arriving from the upper left which causes a phase difference between the antennas.

ming. Direction Finding makes use of the amplitude and phase characteristics of a signal at multiple receive antennas. Figure 8 shows the NOAA-CODAR approach using 4 antennas in a square with $\lambda/2$ or slightly less diagonal distance. An echo directed from the upper left in the figure arrives at the 4 antennas with a short time delay, which can be measured as a phase difference. Signals coming from different directions are identified by a changing set of phase differences.

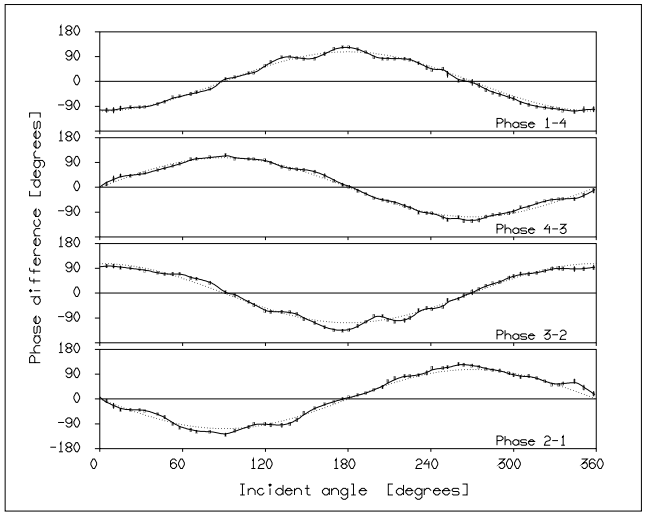


**Figure 10.** The measured phase differences for the antenna array mounted on the A-frame of RV Valdivia.

Figure 9 shows the expected phase differences between the four antennas as a function of incident angle. In this example, the distance between the antennas is slightly reduced from $\lambda/2$ (180°) to 150° for better mounting of

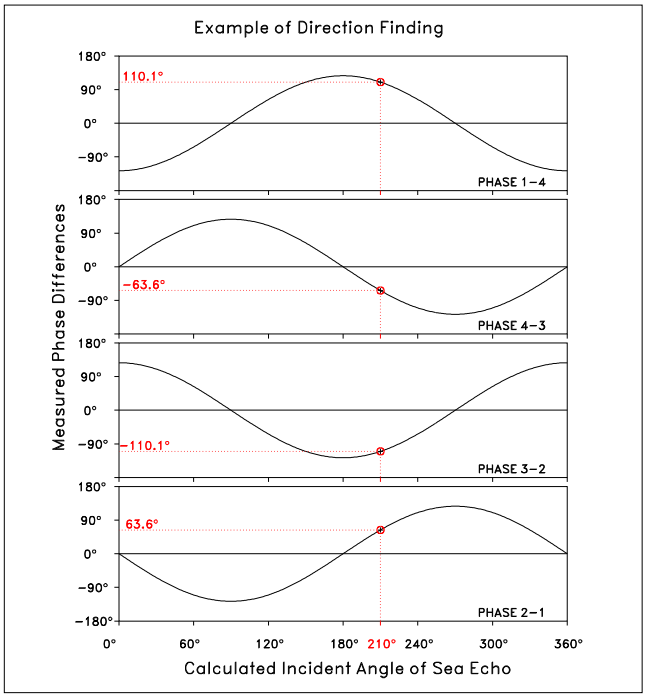


**Figure 9.** How to find the incident angle from the measured phase differences.

the array on RV Valdivia's A-frame. Figure 10 shows the phase differences of the array installed on RV Valdivia as a function of incident angle. These functions have been measured during a calibration procedure and include the distortion due to the ship's body.

To find the incidence angle of a signal, a least-squares-fit of the measured phase differences to the calibrated phase functions is applied:

$$\varepsilon(\Theta) = \sum_{i=1}^{4} (\min(|\,\varphi_i^\star - \varphi_i(\Theta)\,|\,, 360 - |\,\varphi_i^\star - \varphi_i(\Theta)\,|))^2$$

$$\varepsilon(\Theta) \Longrightarrow Minimum$$

with $\varphi_i^\star$ being the measured set of phase difference, $\varphi_i(\Theta)$ being the calibrated values, and $\Theta$ being the incidence angle. The sum $\varepsilon(\Theta)$ goes to a minimum at the most propable incidence angle.

As the antennas receive the echos from all directions simultaneously, all these echos add up to a set of phase differences which can not be resolved to a single direction. However, if these echos represent different surface current velocities, they appear at different Doppler shifts in the spectrum, which splits up the echos in the frequency domain. Going through the spectrum line by line, each signal can be resolved to it's direction. In case of two or more signals at the same Doppler shift coming from different directions, this algorithm fails. Using the measured amplitudes in addition to the phase differences

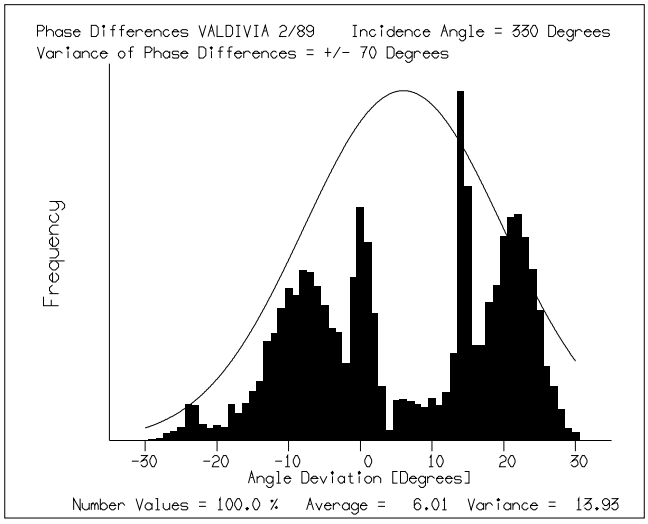


**Figure 11.** The frequency distribution of resolved incident angles using the calibrated phase difference values shown in figure 10. A simulation result showing a worst case.

an algorithm resolving two directions can be formulated. However, in practical applications this algorithm tended to find spurious second directions e.g. on land. This also happened with nearly undistorted antenna patterns of arrays installed on the beach. The best solution to this more-than-one-angle problem is to cut the measured time series into overlaping fractions. The echo statistics vary with time, and the algorithm has the chance to pick up the correct directions from the fractions of the time series.

In some cases the single-angle least-squares solution described above using the calibrated phase differences on board a ship still showed spurious radial current fields. For this reason, a simulation study has been performed: A signal coming from one distinct direction was selected, e.g. 330 degrees incidence angle. Then Gaussian noise has been added to the phase differences with a mean value of zero and the sum of the variances of the four noise values to be a constant value, e.g. 70 degrees. To get a good statistical stability, several thousands of different noise values have been added to the known signal. The results have then been passed through the least-squares algorithm and a statistic of the incident angles resolved has been recorded.

In a first study, the algorithm has been tested with the undistorted antenna patterns. The result was a gaussian frequency distribution of the resolved angles with an average offset of zero.

Figure 11 shows the frequency distribution of the resolved angles using the distorted antenna pattern from the ship-borne array. It can be seen clearly that the distribution found is no longer gaussian and the average shows a resolved incidence angle offset of +6 degrees. Using the measured antenna pattern does not completely overcome the problem to find the correct incidence angle under these conditions. As a consequence, antenna pattern distortions should be minimized.

### *2.4 Azimuthal resolution by Beam Forming*

If access to the second order backscatter from the sea surface is needed, the Direction Finding scheme described above can not be applied. The strong first order Bragg lines from other directions are superposed to the weaker second order signals. A solution is to use a linear antenna array and apply Beam Forming. This technique forms a beam to a distinct direction and allows access to the complete backscatter spectrum from the selected patch of the sea surface. The width of the beam depends on the ratio array length to electromagnetic wave length and is about $\pm 3$ degrees for 16 antennas at $\lambda/2$ spacing. At 30 MHz the array is 75 m long.

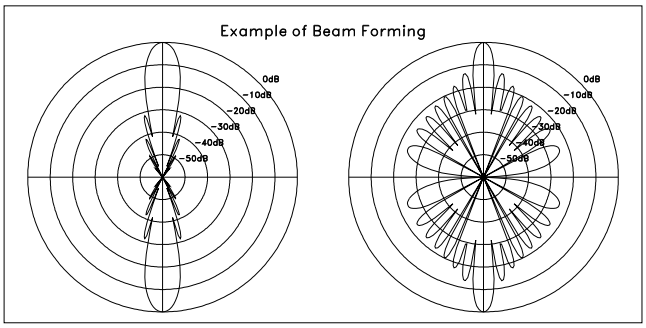


**Figure 12.** The antenna pattern of a linear array with 16 antennas at $\lambda/2$ spacing (right side). A windowing function has to be applied to reduce side lobes (left side).

To reduce side lobes in the antenna pattern, a windowing function has to be multiplied on the amplitudes of the antennas before the signals are shifted in phase to stear the beam and added up finally. A linear array has a large aperture and is quite insensitive against distortions due to the environment. The most sensitive characteristic in this respect is the side lobe suppression. A disadvantage of linear arrays is the large area needed for installation. In addition, it takes much more work to set up all the antennas and cables. However, in many cases the linear array gives more reliable results and for access to the full Doppler spectrum it is mandatory in any case.

## 3 The WERA HF radar

The University of Hamburg WERA HF radar has been developed in 1996 within the EU funded Surface Current And Wave Variability Experiment (SCAWVEX) project. The experience regarding spatial resolution and alasing effects has been included into the design. One main difference to the NOAA-CODAR is the use of FMCW modulation for range resolution. The technical requirements for a clean linear frequency chirp could be solved by using a DDS chip. This was not possible 20 years ago, when only Voltage Controlled Osciallators (VCOs) have been available. This design allowed a narrow receiver bandwidth of about 1 kHz and a slow high-resolution A/D converter while still giving a range resolution down to 300 m.

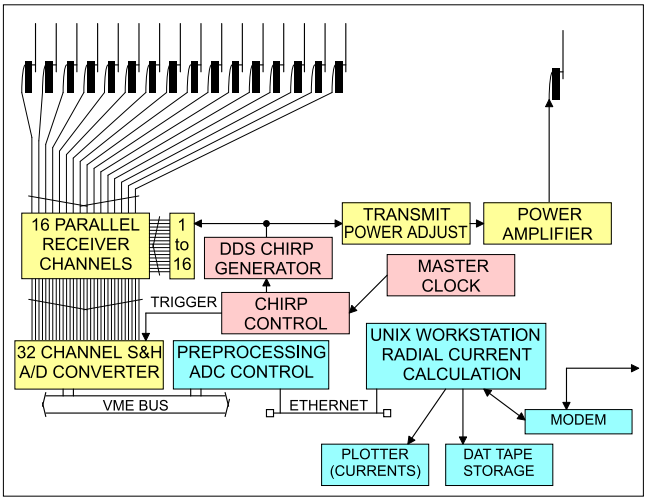


**Figure 13.** The block diagram of the WERA system.

The heart of the system is a low-noise crystal oscillator, which is used as a master clock for all frequency generation and sampling (cf. figure 13). This concept makes the whole system strictly synchronized and coherent. The frequency is doubled to about 180 MHz and then used to clock the DDS. The DDS directly generates the desired working frequency chirp of the radar. Center frequency, bandwidth (giving the range resolution), and duration of the chirp can be programmed by software.

To avoid loss of backscattered energy, the signals received by the antennas are not multiplexed to one receiver. Instead, there is one receiver for each antenna. Amplitude variations and phase shifts between the antennas are measured and compensated by software. Each receiver includes an I/Q demodulator and lowpass filters to avoid aliasing. High dynamic range components have been used to simultaneously handle the strong signal from the direct path and the weak sea echos from far ranges.

Each receiver passes the I- (In phase) and Q- (Quadrature phase) signals to 16 bit low noise A/D converters. The signals from all receivers are sampled simultaneously and passed to a computer system in a sequential way. The computer runs a realtime operating system and processes the range resolving FFTs on-line during the measurement. Azimuthal resolution is provided later on a Unix workstation, where also current vectors and other parameters are processed.

The WERA design is very modular, i.e. when only 4 antennas and receivers are installed, the Direction Finding scheme described above can be used to measure currents with the system. When installing 12, 16, or more antennas and receivers to form a linear array, Beam Forming can be applied and simultaneous measurement of currents and waves will be possibe, just by using different programs on the Unix Workstation.

## 4 Conclusions

The University of Hamburg WERA HF radar has been developed in 1996 and is based on 20 years of experience with development and application of HF radars. It offeres a modular design which can easily be adopted to the requirements of an actual application.

*Acknowledgments.* This work has been partly supported by the European Commission, DG XII, within the Mast-2 programme, project CT94-0103, SCAWVEX (Surface Current And Wave Variability EXperiment) and the Mast-3 programme, project CT98-0168, EuroROSE (European Radar Ocean Sensing). We wish to thank the former members of the HF-radar group, Georg Antonischki and Florian Schirmer, as well as our technician Monika Hamann for their support.

## References

**[1]** D. E. Barrick, M. W. Evans, B. L. Weber, "Ocean surface current mapped by radar", *Science*, vol. 198, pp. 138-144, 1977.

**[2]** H.-H. Essen, M. M. Janopaul, E. Mittelstaedt, J. Backhaus, "Surface currents in the German Bight measured by backscattered radio waves - a comparison with conventional measurements and model results", *North Sea Dynamics* (ed. by Sündermann and Lenz), pp. 159-165, Springer Verlag, 1983.

**[3]** H.-H. Essen, K.-W. Gurgel, F. Schirmer, "Tidal and wind-driven parts of surface currents as measured by radar", *Deutsche Hydrographische Zeitschrift* 36, pp. 81-96, 1983.

**[4]** K.-W. Gurgel, G. Antonischki, H.-H. Essen, T. Schlick, "Wellen radar (WERA), a new ground-wave based HF radar for ocean remote sensing", *Coastal Engineering*, vol. 37, pp. 219-234, 1999.

**[5]** K.-W. Gurgel, H.-H. Essen, S. P. Kingsley, "HF radars: Physical limitations and recent developments", *Coastal Engineering*, vol. 37, pp. 201-218, 1999.

**[6]** E. D. R. Shearman and R. R. Unsal, "Compatibility of High Frequency Radar Remote Sensing with Communications", *IEE Conference Publication No. 188*, "Radio Spectrum Conservation Techniques", pp. 103-107, IEE, London, July 1980.

**Address of the authors:**
Universität Hamburg, Institut für Meereskunde,
Troplowitzstraße 7, D-22529 Hamburg, Germany
Phone: +49 40 42838 5742
Fax: +49 40 42838 5713
Email: gurgel@ifm.uni-hamburg.de
WWW: http://ifmaxp1.ifm.uni-hamburg.de/